Journal of Photochemistry and Photobiology A: Chemistry 343 (2017) 119–125

Contents lists available at ScienceDirect

Journal of Photochemistry and Photobiology A: Chemistry

journal homepage: www.elsevier.com/locate/jphotochem

Airborne nano-TiO_2 particles: An innate or environmentally-induced toxicity?

David Vernez*, Jean-Jacques Sauvain, Alexis Laulagnet, Alejandro Portela Otaño, Nancy B. Hopf, Kiattisak Batsungnoen, Guillaume Suárez

Institute of Work and Health (IST), University of Lausanne and Geneva, Lausanne, Switzerland

ARTICLE INFO

Article history:
Received 22 February 2017
Received in revised form 13 April 2017
Accepted 17 April 2017
Available online 20 April 2017

Keywords:
Nanoparticles
TiO_2
Solar UV
Oxidative capacity
Oxidative stress
Airborne particles

ABSTRACT

Titanium oxide (TiO_2) is a known photocatalyst, able to produce reactive oxygen species (ROS) when exposed to UV light. TiO_2 phototoxicity has been abundantly demonstrated in aqueous solutions. Little is known; however, about its phototoxicity as an aerosol, particularly in the nano-size particle range. An experimental setting was developed to measure the oxidation capacity of TiO_2 NP with or without exposure to UV light. TiO_2 NP were generated using a Collison nebulizer, carried through a diffusion dryer and exposed to UV using the collimated beam of a solar light simulator. Their oxidation capacity was measured on-line via a photonic sensor based on multiscattering absorbance enhancement (MAE) strategy. The oxidative potential of aerosolized TiO_2nanoparticles is exacerbated by exposure to UV light. The oxidative response is affected by humidity and reaches its maximum in the 70%–90% relative humidity range. Gaseous hydrogen peroxide (H_2O_2) was found to be the predominant oxidative specie. Our results suggest that the use of TiO_2 nanoparticles in outdoor environments or close to artificial UV sources lead to an involuntary exposure to ROS, to an extent greater than previously known. It raises also concerns about other environmental pollutants known to be UV photosensitive.

1. Introduction

The titanium oxide (TiO_2) photosensitivity is well known [1]. TiO_2 is photoactivated when exposed to UV light below 390 nm, resulting in photon absorption and excitation of an electron (e^-) thereby generating a positive electron hole (h^+) in the valence band [2]. The photogenerated electrons react with molecular oxygen (O_2) to produce superoxide radical anions ($O_2^{\bullet -}$), while the holes react with water to produce hydroxyl radicals ($HO^\bullet$) [3]. These properties make TiO_2 a popular photocatalyst and, less fortunately, a potential phototoxicant.

In the nano particulate (NP) range this photocatalytic reactivity is further enhanced as the relative surface area increases, promoting the extensive industrial use of TiO_2 NPs in applications such as nanocrystalline solar cells, self-cleaning and antibacterial paintings or cements and coatings. TiO_2 NPs are present in thousands of consumer and professional products including sun screen. To reduce the generation of reactive oxygen species (ROS) within the sunscreen and consequently adverse phototoxic effects on the skin, the TiO_2 NPs have to be coated with inert silica [4].

In the last decade, hundreds of studies have reported on the increased incidence of lung injury and pulmonary inflammation induced by exposure to TiO_2 NPs [5]. The deleterious effects of TiO_2 NPs are strongly associated to ROS generation [5,6]. This ROS generation induces pulmonary inflammatory response in a dose-dependent manner, and is involved in oxidative stress-mediated signalling events affecting all characters of cancer cell behavior [7,8].

The phototoxicity of TiO_2-NPs particles in aqueous solutions has been evidenced on aquatic species such as zebrafish embryos [9], on aquatic benthic organisms (Hyalella azteca) [10], or on bacteria (Escherichia coli and Aeromonas hydrophila) [11]. It has been argued that, without considering its photoactivity, the toxicity of TiO_2-NPs could be largely underestimated [12]. It was hypothesized that the role of the intrinsic physico-chemical properties of the nanoparticles (e.g. size, morphology, band gap) were playing an essential role in their phototoxicity [10]. Although well known in aqueous solution the phototoxicity of TiO_2-NPs as aerosolized

* Corresponding author at: Institute of Work and Health (IST), rte de la Corniche 2, 1066 Epalinges-Lausanne, Switzerland.
E-mail addresses: david.vernez@hospvd.ch (D. Vernez), jean-jacques.sauvain@hospvd.ch (J.-J. Sauvain), alaulagnet@gmail.com (A. Laulagnet), alejandro.portela-otano@chuv.ch (A.P. Otaño), nancy.hopf@hospvd.ch (N.B. Hopf), kiattisak.batsungnoen@unil.ch (K. Batsungnoen), guillaume.suarez@chuv.ch (G. Suárez).

http://dx.doi.org/10.1016/j.jphotochem.2017.04.022

particles is poorly described. Some studies have shown that TiO_2 surfaces irradiated with UV light can produce ROS in air [13]. While the production of $HO^{\cdot}$ has been found to be a key mechanism in water, alternative reactions pathways prevails in the gaseous phase due to the presence of molecular oxygen [14]. Species such as superoxide radical $\left(O_2^{-\bullet}\right)$, singlet oxygen $^1O_2$ and hydrogen peroxide H_2O_2, in the presence of humidity, have been identified as by-products of the decomposition of molecular oxygen.

The ROS producing capability of airborne TiO_2 NPs with or without concomitant exposure to UV and the possibility of generating oxidation in a remote medium have been investigated in this study using a recently developed photonic sensor [15]. A possible generation of airborne photo toxicity would raise concerns about the use of TiO_2 NPs containing materials in outdoor environments or close to an artificial UV source. Airborne ROS species could indeed reach the pulmonary system in exposed individuals and generate a potentially harmful oxidative stress.

2. Method

2.1. Experimental setup

The overall setup shown in Fig. 1 was used to: (i) generate several airborne concentrations of TiO_2 NP under controlled relative humidity levels; (ii) expose TiO_2 NP aerosols to UV light at constant flow rate; (iii) assess on-line the corresponding ROS levels produced.

The Collison nebulizer containing 100 mL of aqueous suspension of TiO_2 NP was fed with dry air (2 bar) with the flow rate ν_{tot} = 1.7 L/min. The generated aerosol was driven to the diffusion dryer where RH was controlled by adjusting the silica-gel filling. TiO_2 NP aerosol stream was introduced, at controlled RH, into the vertical exposure tube (glass; L = 90 cm; cross-section area: 104 cm^2) located right under the collimated UV light beam (open top part of the tube is sealed to the lens of the lamp with silicon). The flow rate ν_{tot} was constant and the period of UV exposure for TiO_2 NP was about 5.5 min. The travel time of the aerosol (particles + gas) between the exposure tube and the measurement cell was of about 10 s. The photonic sensor system based on multiscattering absorbance enhancement (MAE) measures ROS through the progressive oxidation of the Fe(II)-containing assay solution known as FOX The resulting color change is expressed as the time variation of a dimensionless normalized coefficient, ΔG. Calibration of the sensor system enables the conversion of $\Delta\Gamma$ values obtained under various experimental conditions into amounts of produced H_2O_2 equivalents (nmol).

2.2. Photonic sensor for oxidation capacity determination

2.2.1. Photonic sensor principle

The oxidation capacity of TiO_2 aerosols was determined on-line via a photonic sensor recently developed in our laboratory based on multiscattering absorbance enhancement (MAE) strategy. The sensor principle relies on the use of a random medium, such as microbeads, glass fibers or cellulose membrane, inserted in the optical cell with the aim to lengthen the optical path under multiscattering regime (Fig. 2). A gain in sensitivity is obtained as the absorbance signal of a given molecule is dramatically enhanced [16,17]. The optical cell used in this study was made of a glass tube (diam. 5 mm) in which a rolled piece of cellulose membrane (10 × 15 mm) was inserted to act as absorbance enhancer. The

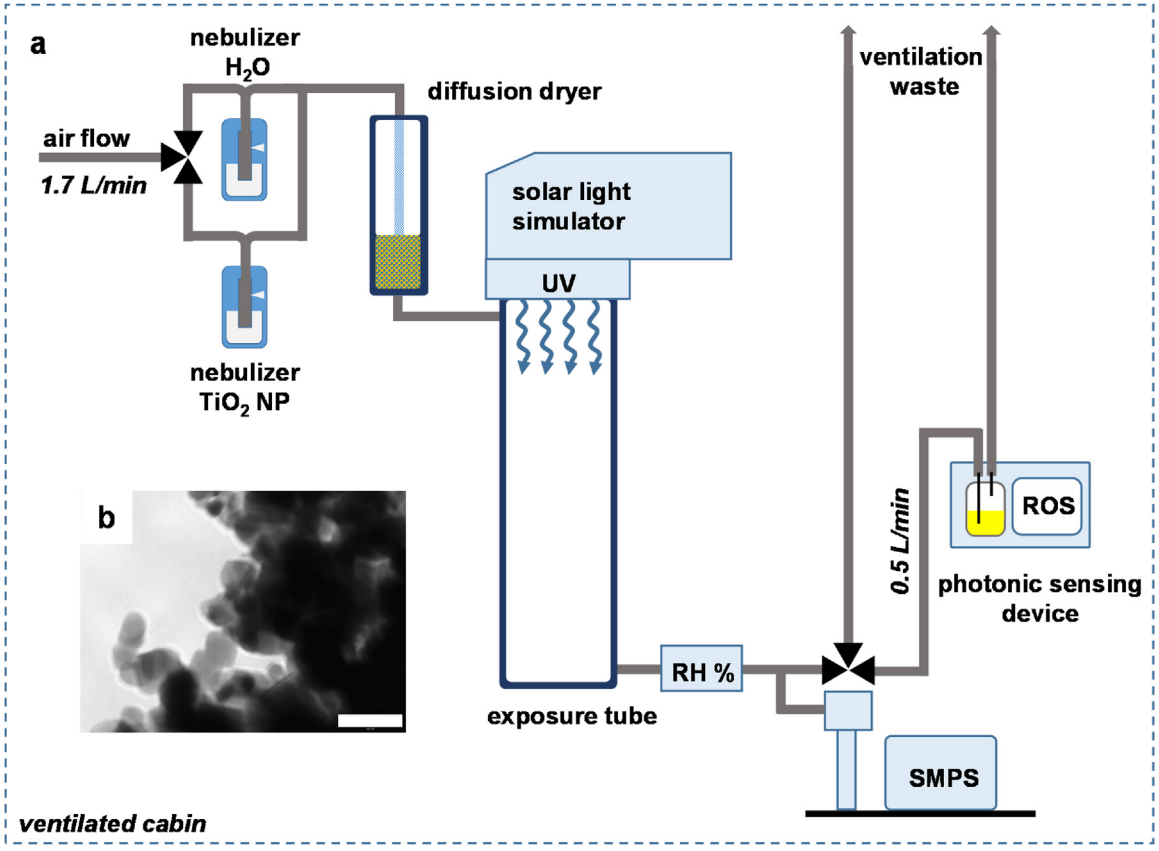

Fig. 1. Experimental setup for the generation of TiO_2 NP aerosol and on-line quantification of photo-induced ROS. a, Flow line schematic of the experimental setup showing TiO_2 aerosol produced via nebulizer reaching continuously the UV-exposure tube under controlled humidity (adjustable dryer) and the photonic sensing device enabling real-time ROS detection. b, TEM image of TiO_2 NP (Aerosil TiO_2 P-25) aerosolized in the system. Scale bar, 50 nm.

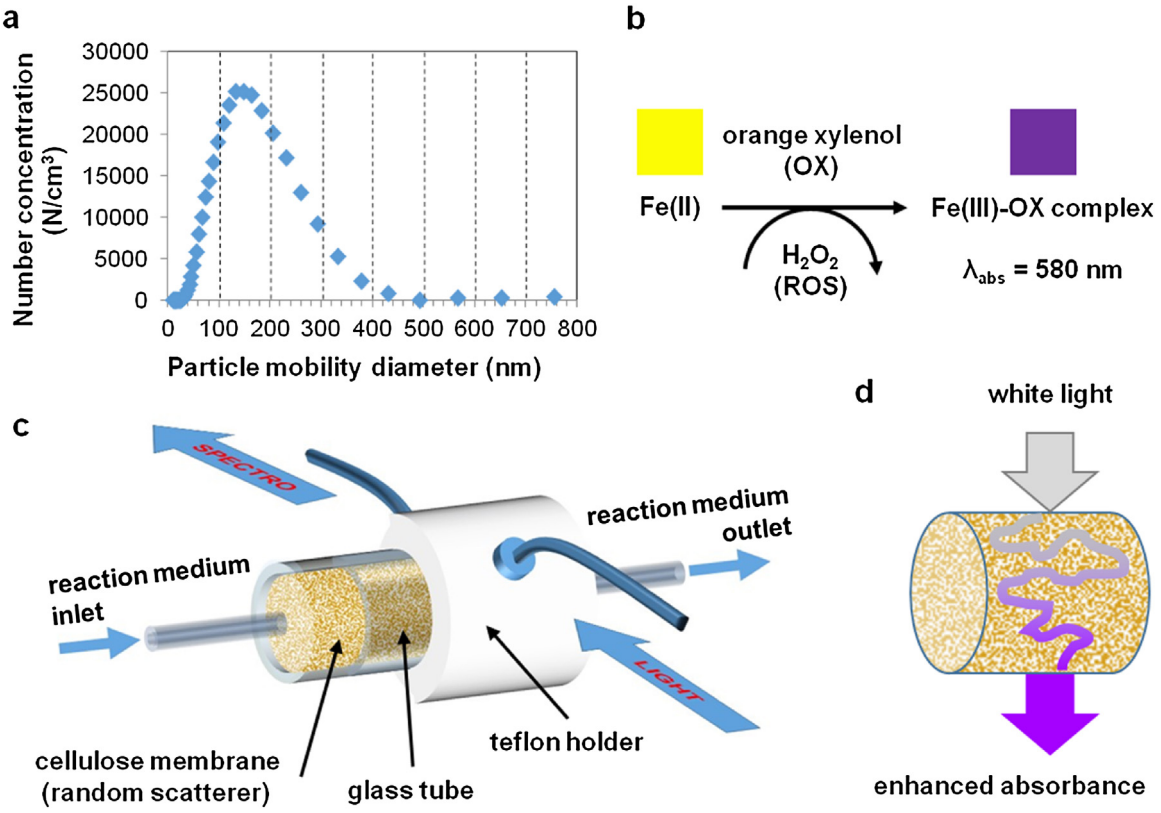

Fig. 2. Airborne TiO_2 NP size characterization and ROS sensing approach. a, TiO_2 aerosol size distribution obtained with scanning mobility particle sizer exhibiting a modal diameter of about 150 nm. b, schematic describing the principle of FOX colorimetric assay in which ROS induce the change in absorbance at 580 nm. c, Schematic drawing of the photonic sensing cell containing the cellulose membrane that enhances the measured absorbance. The continuous circulation of sample-bubbled FOX solution through the sensing cell enables real-time ROS quantification. d, Schematic representation of the multiscattering absorbance enhancement strategy where light propagation through a random medium (*ie* cellulose membrane) considerably lengthens the optical path and therefore the measured absorbance.

developed MAE-based sensor was coupled to a standard colorimetric FOX-sorbitol assay. This colorimetric assay briefly relies on Fe(II) oxidation by ROS and subsequent formation of xylenol orange-Fe(III) violet complex. Furthermore, the presence of sorbitol chemically enhances the reaction via the formation of radical intermediates. During measurements the FOX solution maintained at 20 °C circulates in close loop from the reaction vial, where the aerosol sample was introduced via bubbling, to the optical cell. The spectral changes of the incoming light propagating through the optical cell were continuously registered with the compact spectrometer in the visible range (integration time = 7s). Spectral analysis was performed in order to calculate a dimensionless normalized coefficient, Γ, expressed as:

$$\Gamma = \left(\frac{I_{580} - I_{700}}{I_{700}}\right)_t \Big/ \left(\frac{I_{580} - I_{700}}{I_{700}}\right)_{t0} \Gamma$$
$$= \left(\frac{I_{580} - I_{700}}{I_{700}}\right)_t \Big/ \left(\frac{I_{580} - I_{700}}{I_{700}}\right)_{t0}$$

Where I is the light intensity measured at the sensing (580 nm) or reference (700 nm) wavelengths.

2.2.2. Photonic sensor characterization

The calibration and performance of the ROS sensor system was described in a previous publication [15]. In short, it is calibrated by adding known amounts of H_2O_2 ranging from 40 pmol to 4 nmol in the reaction vial (4 mL) containing the FOX solution (reaction mixture: 2.7 mL FOX and 1.3 mL H_2O_2 standard). At any time of the reaction the change in the calculated Γ, $\Delta\Gamma = \Gamma t_0 - \Gamma t$, was found to increase linearly with H_2O_2 concentration. The limit of detection was estimated to be of 9 nM H_2O_2 from the calibration curve analysis (LoD = 3σblank*slope). In the absence of MAE, the LoD was found to be 121 nM H_2O_2, indicating that the analytical performance of the sensor was improved by one order of magnitude.

2.3. On-line determination of ROS in TiO_2 aerosol

TiO_2 aerosol sample (or clean air as background) was continuously introduced by bubbling (flow rate: 0.5 L/min) in the reaction vial containing the reaction mixture (FOX solution and water; 2:1 vol:vol) circulating in close loop through the system via the sensing cell. The sampling efficiency of the bubbling was calculated at 42% for H_2O_2 at the used experimental conditions. Therefore, all the measured oxidation capacity values have to be considered as equally underestimated. The established calibration curve enabled the conversion of raw experimental curves ($\Delta\Gamma$ vs time) into oxidation curve that show the time evolution of H_2O_2 equivalents (nmol) produced in the system. Similarly, linear sections of the obtained curves corresponding to steady-state regime of the reaction were converted into oxidation capacity expressed in nmol/L_{air}. Between each experiment the cellulose membrane insert was replaced in the sensing cell and conditioned for 30 min with circulating reaction mixture.

2.4. ROS speciation experiments

The presence of $OH^\bullet$ in the gaseous phase was assessed using the benzoate probe, as described by [18]. The generated $OH^\bullet$ reacts quantitatively with the benzoate anion (BA), producing the *p*-hydrobenzoate (*p*-HBA) which was quantified by UV at 256 nm.

A solution of benzoic acid 2.8 mM was prepared in ultrapure water. The whole TiO_2 NP aerosol was aspirated at a flow rate of 0.3 L/min through an impinger filled with 4 mL of the BA solution during 80–145 min. The resulting solution was filtrated through a 0.2 μm Teflon filter then injected (10 μL) on an HPLC system. The elution was done in an isocratic mode with 70% H_2O set at pH 2 with $HClO_4$ and 30% acetonitrile at a flow of 0.6 L/min. The limit of detection for the *p*-HBA with this method has been determined to be about 0.15 μM.

The detected values for *p*-HBA obtained for two independent generations were found to be below the limit of detection, suggesting that the production of $OH^\bullet$ was lower than 4.8 nmol during the sampled time [18].

Similarly, H_2O_2 was quantified by introducing the whole UV exposed TiO_2 NP aerosol at a flow rate of 0.5 L/min into a 10 mL impinger filled with ultrapure water, for 15 min. The resulting sample was analysed using FOX assay adapted to 96-wells microplate format. In this assay, each well was filled with 133 μL of FOX solution and 67 μL of sample and let to react for 20 min (reaction maximum) before reading. The calibration was performed by adding H_2O_2 concentrations ranging from 0 to 10 μM to the FOX solution. The limit-of-detection was estimated to be about 0.16 μM.

Reagents and materials: available in Supplementary material S1.

3. Results & discussion

The analysis of the experimental oxidation curves representing the time evolution of produced H_2O_2 equivalents per volume of aerosol sample (nmol/L_{air}), defined as oxidation capacity, provides a direct information on the reactivity of the generated airborne samples although the absolute values are equally underestimated. The steeper the curve slope is, the faster the oxidation process takes place, indicating an increased capability of the incoming aerosol sample to generate ROS.

Stable oxidation signal and background levels were reach for each experiment after bubbling clean air into the measurement cell for 1500–3000 s. The effect of increasing dissolved molecular oxygen levels in the sensor system was clearly shown with a mean background oxidation capacity of 0.115 (SD 0.062) nmol/L_{air}. This initial "air only" period, was systematically deduced from each experimental oxidation curve, resulting in a background-corrected flat response. Airborne TiO_2 NPs particles (250′000 [N/cm^3]) were introduced into the system with or without concomitant UV radiation exposure. In both measurements, an airborne concentration of about 250′000 [N/cm^3] of TiO_2 NPs was used. The slope of the corresponding oxidation curves (Fig. 3a) measured after introduction of TiO_2 NP (red curve) and UV-exposed TiO_2 NP (blue curve) in the system were $5.4 \cdot 10^{-4}$ and $2.2 \cdot 10^{-3}$ nmol/s, respectively (*ie* an oxidation capacity of 0.065 and 0.265 nmol/L_{air}). Several seconds after UV light exposure (t = 330 s, irradiance) had stopped, the aerosolized TiO_2 NPs still exhibited a four-fold increase in oxidative capacity compared to the TiO_2 NP that had not been irradiated with UV light.

3.1. Characterization of the ROS species

Further experiments were performed to determine whether the ROS produced upon photocatalysis remained adsorbed to the TiO_2 NP surface or diffused away through the air. The aerosol (the UV exposed TiO_2 NP) and gas phases were separated using an on-line mechanical filtration (HEPA filter), and the remaining air stream analysed (Fig. 3b). In this experiment, an initial concentration of about 280′000 [N/cm^3] of TiO_2 NPs was introduced into the system. A steep increase in the oxidation curve was observed when particles were exposed to UV light (purple curve). When introducing a HEPA particle filter downstream to the UV irradiation area and upstream from the detection device, a clear oxidative response was still observed (blue curve). SMPS measurements showed that the HEPA filter reduced the particles concentrations to negligible levels (<30 [N/cm^3]). Additionally, no oxidation capacity was observable when the filter was used without the UV light (orange curve), indicating that no oxidative species is present in the gas phase alone. This finding points out that the oxidation capacity observed in the absence of UV for the whole aerosol (Fig. 3b) is due to oxidative species adsorbed at the TiO_2 NP surface. The oxidative response observed with the filter and UV light was in the range of the one observed without filter and with UV, suggesting that a majority of the ROS was in the gas phase and not adsorbed onto the particle surface. Moreover, the chemical speciation of photocatalytically produced ROS conducted on UV-irradiated TiO_2 NP aerosol indicated the presence of H_2O_2 but no hydroxyl radicals were detected (Supplemental material). The measured concentration for H_2O_2 was about 0.17 nmol/L_{air} while it was below the limit of detection for $OH^\bullet$ (<0.06 nmol/L_{air}). The oxidative capacity induced by the TiO_2 NP aerosols was therefore predominantly attributable to the H_2O_2 present in the gas phase. These results are coherent with previous findings [19]. The H_2O_2 released in the gas phase was able to induce a remote oxidation of a solid surface that was not in contact with the TiO_2. The long lifetime of airborne H_2O_2, (10^4 s [20]), suggests that the oxidative capacity of the aerosol (particles and gas) will remain effective long after UV exposure stops.

UV irradiation chemistry at TiO_2 surface results in the formation of a pair of valence band hole (h^+) and conduction band electron ($\bar{e}$). Hydroxyl anions and water molecules present at the surface act as h^+ trap, resulting in the generation of highly reactive hydroxyl

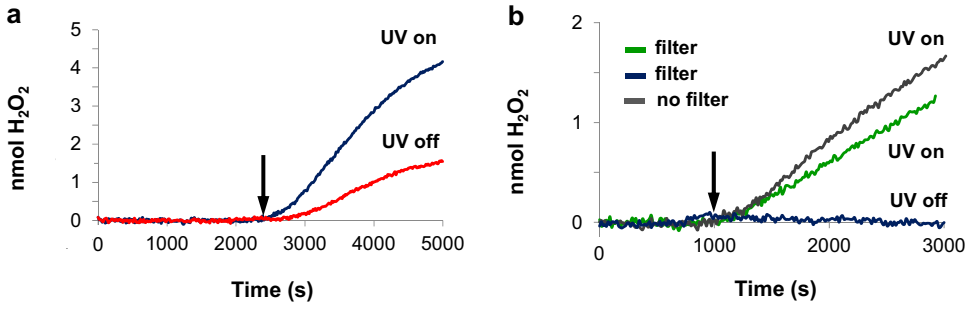

Fig. 3. Real-time quantification of ROS levels, expressed in H_2O_2 equivalents, produced by TiO_2 NP aerosol under controlled UV exposure. a, Oxidation curves induced by UV exposed and non-exposed airborne TiO_2 NPs (concentration 250′000 N/cm^3). b, Oxidation curves induced by UV exposed and non-exposed TiO_2 NPs (concentration 280′000 N/cm^3) measured either in the gas phase (HEPA filter) or in the whole aerosol (no filter). The black arrows indicate the introduction of the particle aerosol in the setting.

radicals that can desorb and diffuse through the surrounding medium [1]. Molecular oxygen represents the main scavenger for conduction band electrons (edge at *ca.* −0.51 V) giving rise to the formation of superoxide anions, $\left(O_2^{-\bullet}\right)$, that remain adsorbed onto the TiO_2 surface. While the contribution of free hydroxyl radicals to the oxidation capacity measured under UV irradiation cannot be discarded [21], our results suggest that its role was not predominant. In most of experimental protocols that focus on UV-induced formation of ·OH, highly alkaline medium (pH > 10) were used. In the present study the TiO_2 NP were kept slightly acidic (pH about 5.8), due to the use of ultrapure water in the nebulized TiO_2 suspension. Additionally to the extremely short lifetime of free hydroxyl radical, a few μs [22], the experimental acidic conditions probably hampers its formation as indicated by the near-zero apparent quantum efficiency of •OH formation measured at pH 3–7 [23].

A recent study by Kwon et al. has shown that under acidic conditions the protonation of sorbed $\left(O_2^{-\bullet}\right)$ leads to hydroperoxyl radicals, $HO_2^{\bullet}$, which exhibit higher mobility and desorb from TiO_2 particles to diffuse through the medium [24]. In our experimental conditions, the predominant radical species appears thus to be $HO_2^{\bullet}$. Considering that H_2O_2 originates from $HO_2^{\bullet}$, the latter mechanism provides a reliable explanation to the presence of free-H_2O_2 away from TiO_2 NP surface. The measured H_2O_2 values in this paper are probably underestimated as a part of the generated peroxide is transformed through a photodissociation process under UV irradiance [25].

3.2. Effect of relative humidity on ROS generation

A series of experiments were performed in which the relative humidity (RH) of the aerosol was varied from 20 to 100%, maintaining the airborne TiO_2 NP concentration in the range of 350′000–750′000 [N/cm^3]. A dryer containing variable amount of desiccant was used to achieve humidity control prior to UV irradiation. Once normalized by the particle number concentration (at 600′000 [N/cm^3]), the obtained oxidation capacity values show a strong dependency on humidity (Fig. 4a). Below 30% RH, the oxidative response was not discernible from the background. The oxidation capacity increased markedly between 20% and 60%; and a steep increase, reaching values above 1 nmol/L_{air}, was observed between 60% and 80%. Above 80% RH, a dramatic decrease was observed. It is worth noticing that water condensation was sometimes observed in the UV exposure glass tube in high moist air conditions. These experiments were reported as 100% RH in Fig. 4a. The dependency of the photocatalytic behavior of airborne TiO_2 NP on relative humidity provided insight to which ROS generation mechanism predominated under the study conditions.

Considering, the observed photocatalytic generation of hydrogen peroxide, and assuming that dissolved O_2 represents the limiting factor of the photocatalytic reaction, one would expect a linear relationship with humidity. The non-linear increase of the oxidation capacity with the relative humidity might be partly due to an isotherm regime disruption. The first increase segment corresponding to relative humidity ranging from 20 to 60% can be attributed to the progressive formation of water monolayer until saturation followed by multilayer formation. When RH is further increased, from 60 to 90%, a regime transition from adsorbed layer to capillary bridges formation as described for SiO_2 particles of similar sizes might take place [26]. The steeper increase of oxidation capacity observed in this RH range might be explained by the greater water confinement in the formed capillary bridges between several TiO_2 NPs (Fig. 5). Particularly, the formation of a hydroperoxyl radical-water complex is favored in these conditions and could explain the enhancement of the H_2O_2 production [25]. An additional explanation might be due to the lower water-air interface in the interstitial region that causes the accumulation of hydroxyl radicals and its conversion into H_2O_2. Those mechanisms might contribute significantly to the overall oxidation capacity response. Finally, the fast decrease in oxidation capacity measured for RH > 90% may be due to a light-scattering effect induced by water droplets and/or to the dissolution of the gaseous H_2O_2 into the water droplets condensed on the surface of the exposure tube.

3.3. Relationship between amount of airborne TiO_2 NP and ROS generation

Repetitive measurements of ROS production were conducted with varying the concentration of TiO_2 NP particles in order to further substantiate the effect of UV light. Fig. 4b summarizes these results in comparing the oxidation capacities —obtained with and without UV light irradiation as a function of TiO_2 NP concentration [N/cm^3]. Oxidation capacity values obtained under high (70–90% RH) and moderate level of ambient humidity (50–60% RH) were reported separately. At low NP concentrations

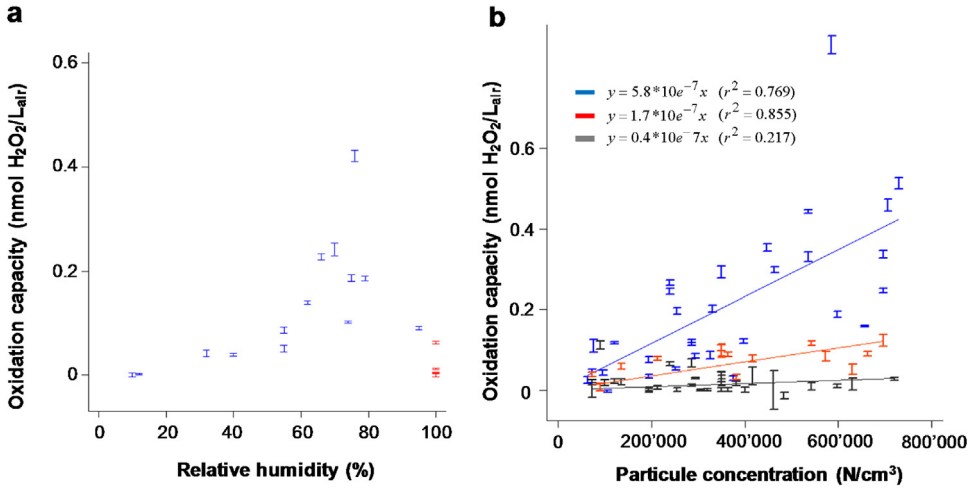

Fig. 4. Effect of humidity conditions and TiO_2 NP concentration on the UV-induced ROS levels. a, Oxidation capacity of TiO_2 NPs exposed to UV light (concentration normalized at 600′000 N/cm^3) in various relative humidity conditions. ■ bars correspond to experimental conditions where condensation took place on the tube. b, Oxidation capacity induced by airborne TiO_2 NPs according to their concentration (particle count): UV exposed – 50–60% RH (■), UV exposed – 70–90% RH (■), non-exposed – 50–90% RH (■). The 5th–95th CI range of the slope estimate is shown for each measurement.

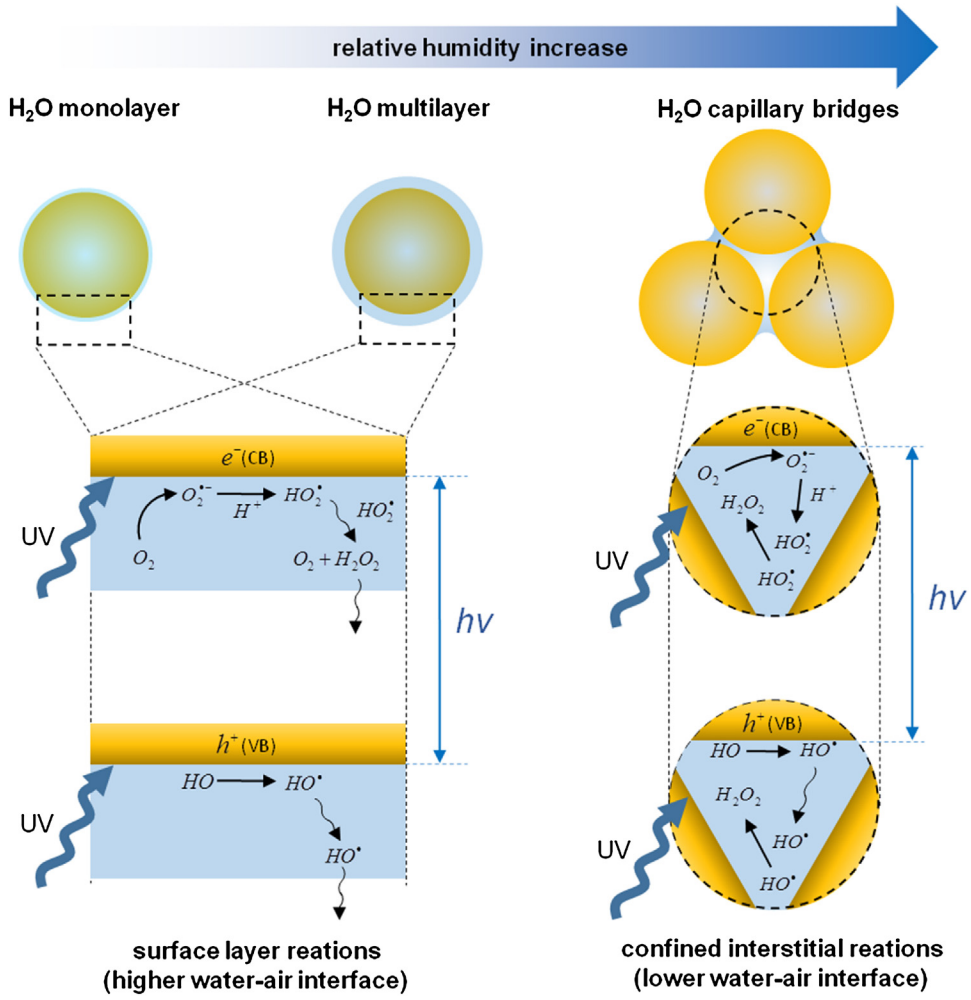

Fig. 5. Proposed mechanism for UV-induced ROS generation on TiO_2 NP aerosol depending on humidity conditions. At low humidity hydrogen peroxide predominantly originates from molecular oxygen reacting with the conduction band electrons (e^-) while hydroxyl radicals formed at the valence band hole (h^+) desorb from the particle surface and can diffuse to the surrounding medium (higher water-air interface). In contrast, at high humidity (RH > 60%) the formation of capillary bridges might happen leading to the confinement of the produced hydroxyl radicals at the interstitial region (lower water-air interface) promoting their recombination into additional hydrogen peroxide.

(<100′000 N/cm^3), no clear distinction could be made between UV-exposed and non-exposed particles; whereas at high NP concentrations, a clear ROS generation was observed. Beyond 100′000 N/cm^3 UV-exposed TiO_2 NP clearly exhibited a higher oxidation capacity that non-exposed particles. Both humidity and particle concentration play a key role in the ROS production. While a significant increase of the oxidation capacity of airborne TiO_2 NP was observed under moderate humidity conditions, a stronger increase is observable at high humidity levels, in agreement with the RH dependency described previously. The relatively high variability observed in oxidation capacity could be attributable to the existing RH variability within each measurements category. Since TiO_2 photocatalysis is a surface-related phenomenon, results were also computed according to the approximate surface of the TiO_2 NP [m^2] assuming a spherical shape. Both particle concentration- and surface- curves exhibits similar profiles (results not shown).

Correlations were calculated, hypothesizing a linear relationship between oxidative capacity and the particle count. The slope of the linear fit was $3.99 \cdot 10^{-8}$, $1.74 \cdot 10^{-7}$ and $5.8 \cdot 10^{-7}$ [nmol cm^3/L$_{air}$] (oxidation slope/part. concentration see Fig. 4b) for non-exposed, UV-exposed at moderate HR and UV-exposed at high HR conditions, respectively. A 4.3 and 14.5 time increase in oxidative capacity was observed between non-exposed and UV-exposed TiO_2 NP at moderate and high%RH conditions, respectively. It should be noted, however, that the slope estimate for the non-exposed particles was approximate because of the low values observed.

The growing use of TiO_2 NP in professional and consumer products, could lead to a large number of exposed individuals. TiO_2 NP issued from the handling of NP-containing powders or from other emissive processes (e.g. wear and tear of a nanoparticles-containing material) would remain in the breathing zone of the users during several minutes. In outdoor situations or in the vicinity of an artificial UV light, this could lead to a potentially harmful ROS exposure. Interestingly, mask filters, commonly used to protect the respiratory system against solid particles aerosols, will not be effective in this case as the H_2O_2 is mostly in the gas phase.

4. Conclusions

This study demonstrated that under environmental conditions, in terms of irradiance, temperature and relative humidity, a UV-irradiated aerosol of TiO_2 NP was responsible for the release of free-diffusing H_2O_2 reaching values up to about 1 nmol/L$_{air}$. This lead to 4.3 and 14.5 times increase in the oxidation potential of the aerosol in moderate and high humidity conditions, respectively.

Our findings highlight the necessity (1) to reconsider the use of non-coated TiO_2 NP in UV exposed environments and (2) to include, additionally to the physical and chemical determination of nanoparticles, the measure of hydrogen peroxide as concomitant and persistent secondary toxicant, within the exposure assessment process. A better measure of ROS generation might help in identifying exposed populations and guide the selection of protection offered to exposed individuals (protection against gases or particulates). More broadly, this raises the question of the role UV plays in the oxidative potential of some airborne pollutants. How much is due to the innate physico-chemical property of the pollutants and how much is due to its UV and humidity environmental conditions? Environmental pollutants such as diesel exhaust, which contain known UV-sensitive species such as polycyclic aromatic compounds should be considered.

Acknowledgements

The authors would like to thanks the research team of Prof. L. Applegate, from Lausanne University Hospital, for kindly providing the UV solar simulator.

This research did not receive any specific grant from funding agencies in the public, commercial, or not-for-profit sectors.

Appendix A. Supplementary data

Supplementary data associated with this article can be found, in the online version, at http://dx.doi.org/10.1016/j.jphotochem.2017.04.022.

References

[1] H. Park, H. -i. Kim, G.-h. Moon, W. Choi, Photoinduced charge transfer processes in solar photocatalysis based on modified TiO2, Energy Environ. Sci. 9 (2) (2016) 411–433, doi:http://dx.doi.org/10.1039/C5EE02575C.
[2] D. Dvoranova, Z. Barbierikova, V. Brezova, Radical intermediates in photoinduced reactions on TiO2 (an EPR spin trapping study), Molecules 19 (October (11)) (2014) 17279–17304.
[3] A. Fujishima, T.N. Rao, D.A. Tryk, Titanium dioxide photocatalysis, J. Photochem. Photobiol. C: Photochem. Rev. 1 (1) (2000) 1–21 (6/29/).
[4] C. Mendrok-Edinger, in: G. Wypych (Ed.), Focus Technology – Sunscreens in Handbook of UV Degradation and Stabilization, 2nd ed., ChemTec, Toronto, 2015, pp. 349–365.
[5] J. Wang, Y. Fan, Lung injury induced by TiO2 nanoparticles depends on their structural features: size, shape, crystal phases, and surface coating, Int. J. Mol. Sci. 15 (December (12)) (2014) 22258–22278.
[6] H. Shi, R. Magaye, V. Castranova, J. Zhao, Titanium dioxide nanoparticles: a review of current toxicological data, Part. Fibre Toxicol. 10 (1) (2013) 15.
[7] E. Panieri, M.M. Santoro, ROS homeostasis and metabolism: a dangerous liason in cancer cells, Cell Death Dis. 7 (June (6)) (2016) e2253.
[8] G.Y. Liou, P. Storz, Reactive oxygen species in cancer, Free Radic. Res. 44 (May (5)) (2010) 479–496.
[9] O. Bar-Ilan, et al., Titanium dioxide nanoparticles produce phototoxicity in the developing zebrafish, Nanotoxicology 6 (6) (2011) 670–679 (2012/09/01).
[10] S. Li, R.J. Erickson, L.K. Wallis, S.A. Diamond, D.J. Hoff, Modeling TiO nanoparticle phototoxicity: the importance of chemical concentration, ultraviolet radiation intensity, and time, Environ. Pollut. 205 (June 26) (2015) 327–332.
[11] T. Tong, et al., Effects of material morphology on the phototoxicity of nano-TiO2 to bacteria, Environ. Sci. Technol. 47 (21) (2013) 12486–12495.
[12] S. Li, L.K. Wallis, H. Ma, S.A. Diamond, Phototoxicity of TiO(2) nanoparticles to a freshwater benthic amphipod: are benthic systems at risk? Sci. Total Environ. 466–467 (January 1) (2014) 800–808.
[13] Y. Murakami, E. Kenji, A.Y. Nosaka, Y. Nosaka, Direct detection of OH radicals diffused to the gas phase from the UV-irradiated photocatalytic TiO2 surfaces by means of laser-induced fluorescence spectroscopy, J. Phys. Chem. B 110 (34) (2006) 16808–16811 (2006/08/01).
[14] A. Fujishima, X. Zhang, D.A. Tryk, TiO2 photocatalysis and related surface phenomena, Surf. Sci. Rep. 63 (12) (2008) 515–582 (12/15/).
[15] A. Laulagnet, J.J. Sauvain, N. Concha-Lozano, M. Riediker, G. Suárez, Sensitive photonic system to measure oxidative potential of airborne nanoparticles and ROS levels in exhaled air, Procedia Eng. 120 (2015) 632–636 (2015/01/01).
[16] G. Suárez, C. Santschi, G. Plateel, O.J.F. Martin, M. Riediker, Absorbance enhancement in microplate wells for improved-sensitivity biosensors, Biosens. Bioelectron. 56 (2014) 198–203 (6/15/).
[17] G. Suarez, C. Santschi, V.I. Slaveykova, O.J. Martin, Sensing the dynamics of oxidative stress using enhanced absorption in protein-loaded random media, Sci. Rep. 3 (December) (2013) 3447.
[18] H. Jung, B. Guo, C. Anastasio, I.M. Kennedy, Quantitative measurements of the generation of hydroxyl radicals by soot particles in a surrogate lung fluid, Atmos. Environ. 40 (February (6)) (2006) 1043–1052.
[19] W. Kubo, T. Tatsuma, Detection of H2O2 released from TiO2 photocatalyst to air, Anal. Sci. 20 (April (4)) (2004) 591–593.
[20] M.-C. Liang, H. Hartman, R.E. Kopp, J.L. Kirschvink, Y.L. Yung, Production of hydrogen peroxide in the atmosphere of a Snowball Earth and the origin of oxygenic photosynthesis, Proc. Natl. Acad. Sci. 103 (December (50)) (2006) 18896–18899.
[21] V. Diesen, M. Jonsson, Formation of H2O2 in TiO2 photocatalysis of oxygenated and deoxygenated aqueous systems: a probe for photocatalytically produced hydroxyl radicals, J. Phys. Chem. C 118 (19) (2014) 10083–10087 (2014/05/15).
[22] F. Wilkinson, W.P. Helman, A.B. Ross, Rate constants for the decay and reactions of the lowest electronically excited singlet state of molecular oxygen in solution. an expanded and revised compilation, J. Phys. Chem. Ref. Data 24 (2) (1995) 663–677.
[23] H. Liao, T. Reitberger, Generation of free OHaq radicals by black light illumination of degussa (Evonik) P25 TiO2 aqueous suspensions, Catalysts 3 (2) (2013) 418.
[24] B.G. Kwon, J. Yoon, Experimental evidence of the mobility of hydroperoxyl/superoxide anion radicals from the illuminated TiO2 interface into the aqueous phase, Bull. Korean Chem. Soc. 30 (3) (2009) 4.
[25] D.W. Gunz, M.R. Hoffmann, Atmospheric chemistry of peroxides: a review, Atmos. Environ. Part A: Gen. Top. 24 (7) (1990) 1601–1633 (01/01 1990).
[26] B. Torun, C. Kunze, C. Zhang, T.D. Kuhne, G. Grundmeier, Study of water adsorption and capillary bridge formation for SiO2 nanoparticle layers by means of a combined in situ FT-IR reflection spectroscopy and QCM-D set-up, Phys. Chem. Chem. Phys. 16 (16) (2014) 7377–7384, doi:http://dx.doi.org/10.1039/C3CP54912G.